Supplementary Materials

Synthesis and Cytotoxic Activity of *N*-(Purin-6-yl)aminopolymethylene Carboxylic Acids and Related Compounds

Victor P. Krasnov [1,*], Olga A. Vozdvizhenskaya [1], Maria A. Baryshnikova [2], Alexandra G. Pershina [3,4], Vera V. Musiyak [1], Tatyana V. Matveeva [1], Kseniya V. Nevskaya [3], Olga Ya. Brikunova [3], Dmitry A. Gruzdev [1] and Galina L. Levit [1]

[1] Postovsky Institute of Organic Synthesis, Russian Academy of Sciences (Ural Branch), Ekaterinburg 620108, Russia
[2] Blokhin National Medical Research Center of Oncology, Ministry of Health of the Russian Federation, Moscow 115522, Russia
[3] Center of Bioscience and Bioengineering, Siberian State Medical University, Tomsk 634050, Russia
[4] Research School of Chemical and Biomedical Engineering, National Research Tomsk Polytechnic University, Tomsk 634050, Russia

Table of Contents

NMR Spectra

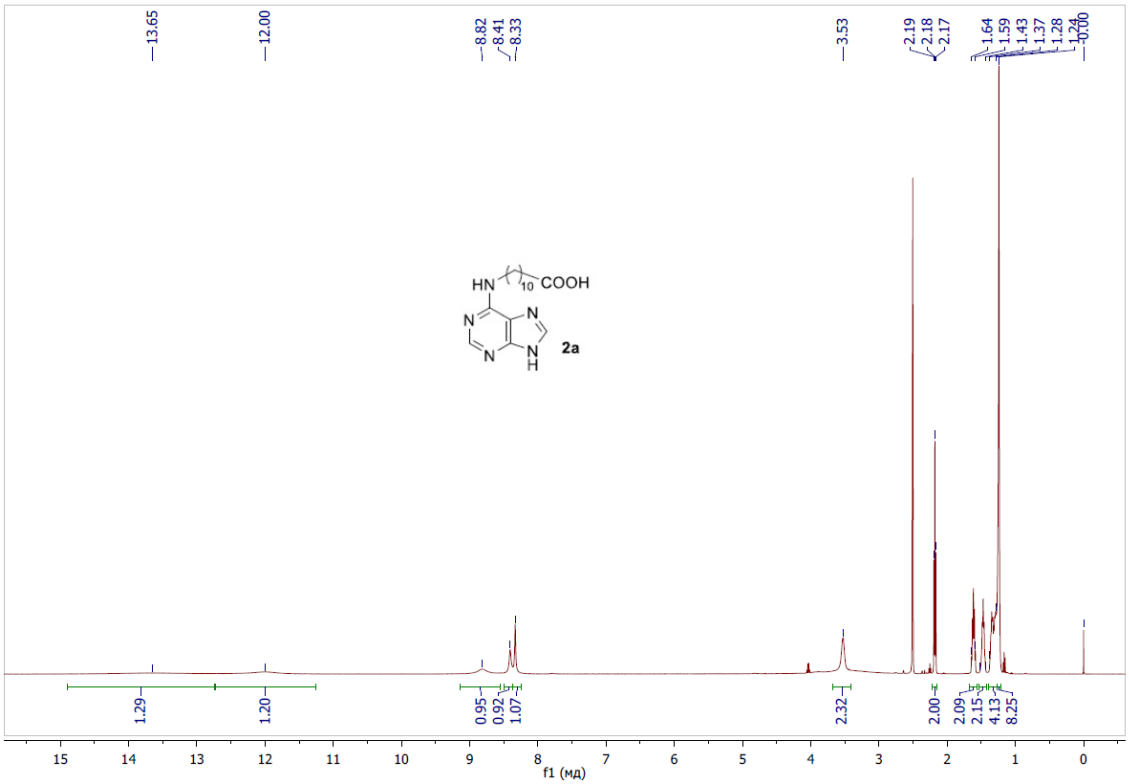

Figure S1. ^{1}H NMR spectrum of compound **2a** (DMSO-d_6, 500 MHz)

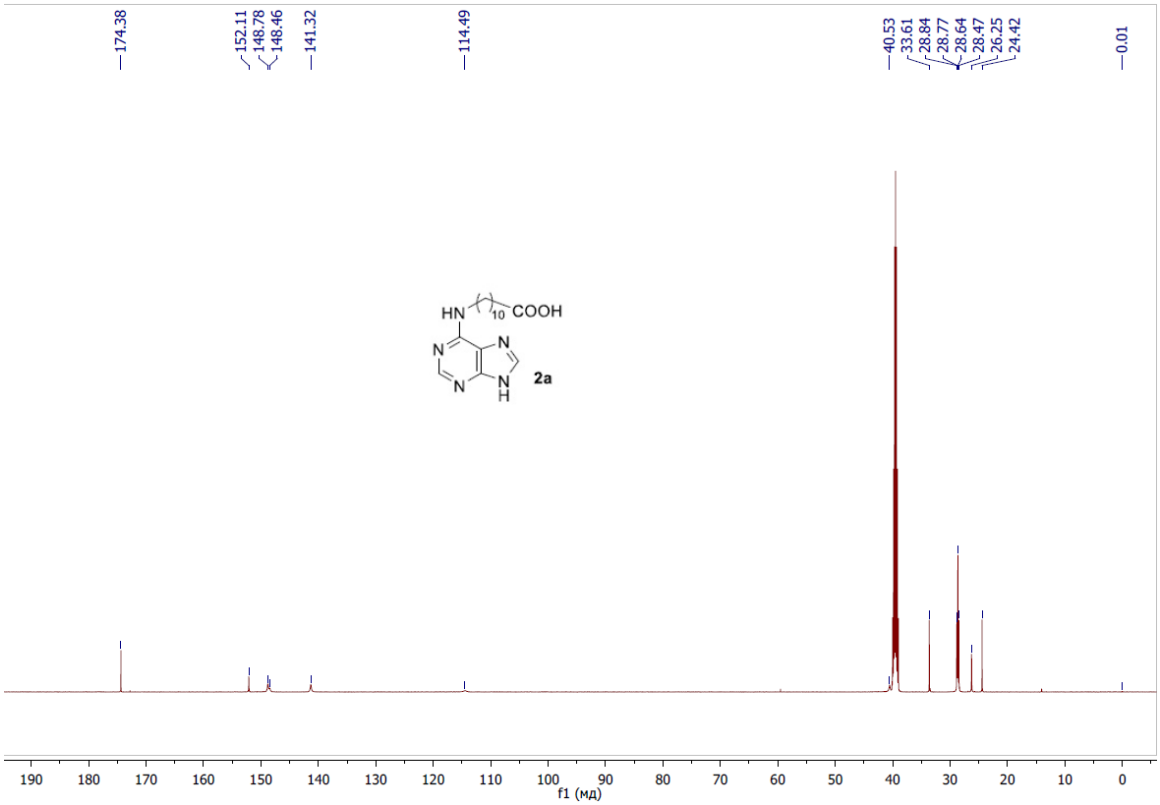

Figure S2. ^{13}C NMR spectrum of compound **2a** (DMSO-d_6, 125 MHz)

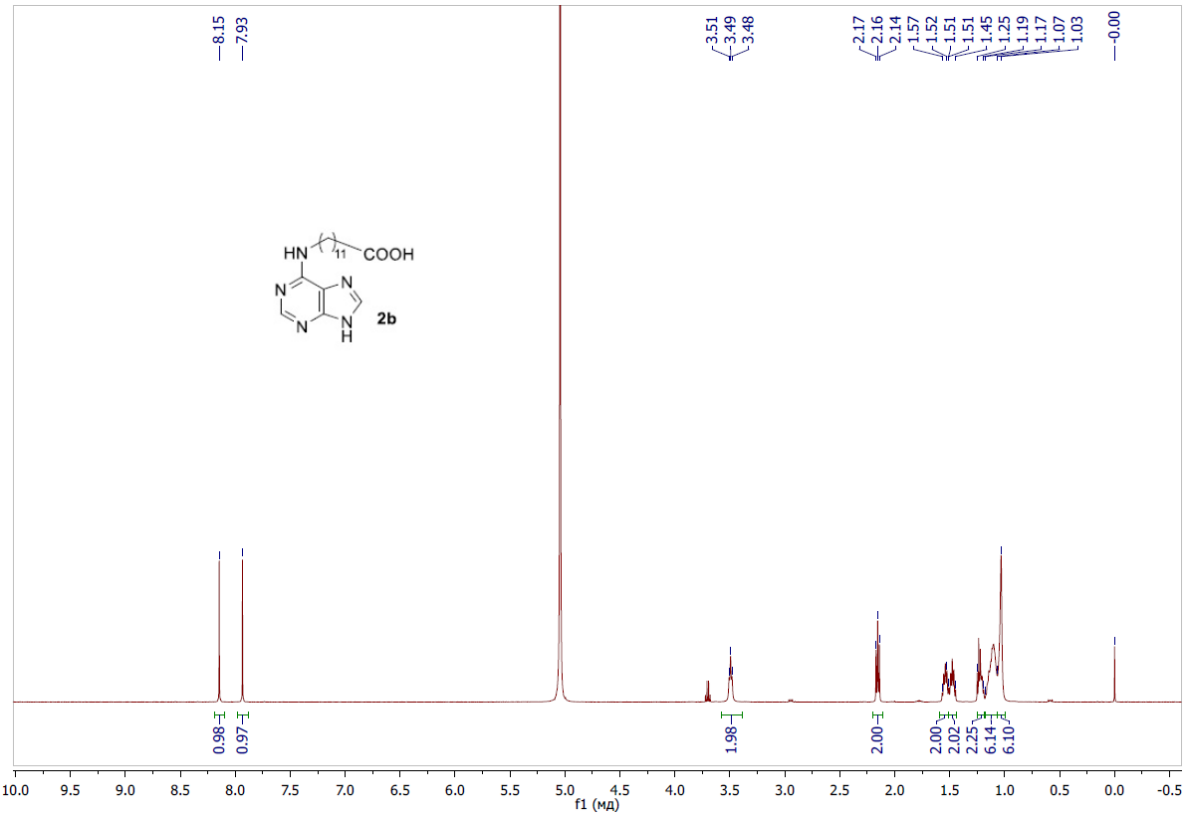

Figure S3. ^{1}H NMR spectrum of compound **2b** (D_2O + NaOD, 500 MHz)

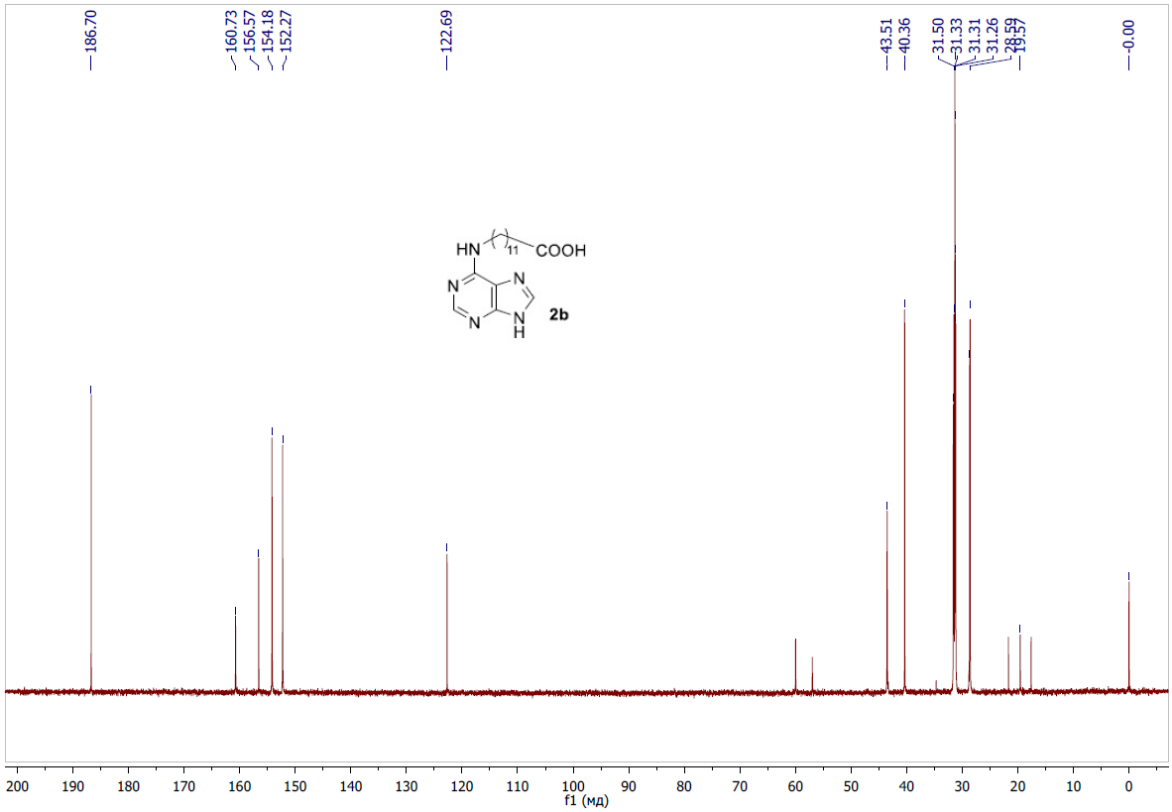

Figure S4. ^{13}C NMR spectrum of compound **2b** (D_2O + NaOD, 125 MHz)

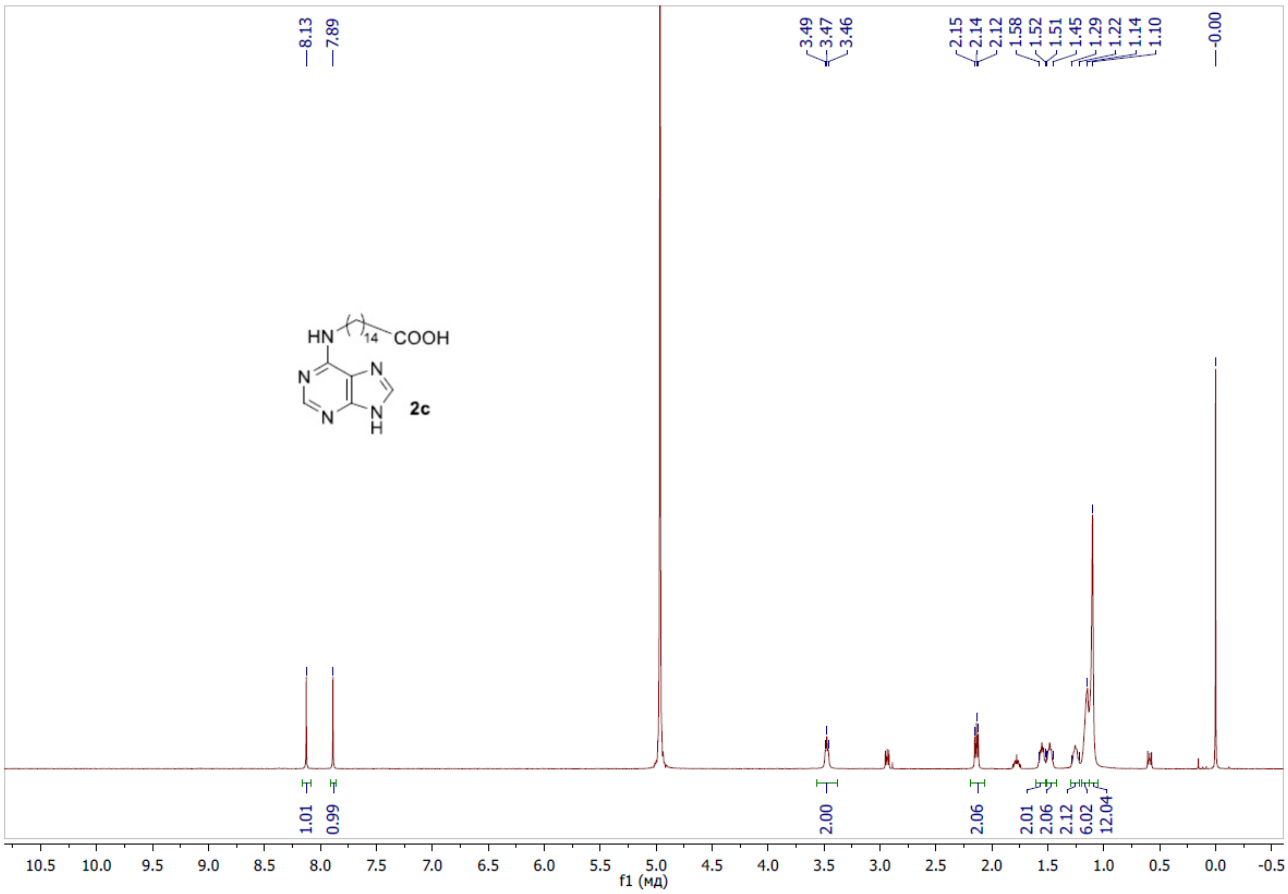

Figure S5. ^{1}H NMR spectrum of compound **2c** (D_2O + NaOD, 500 MHz)

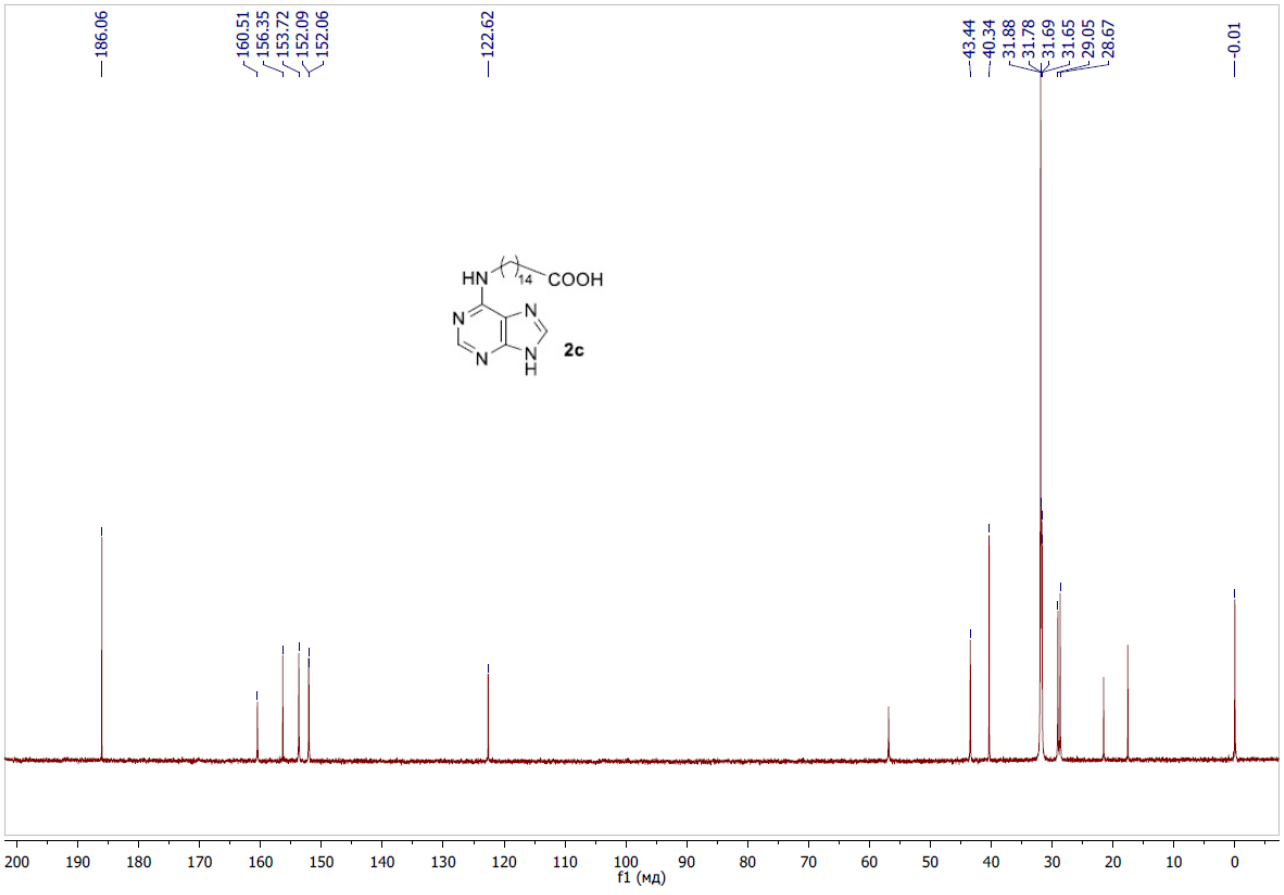

Figure S6. ^{13}C NMR spectrum of compound **2c** (D_2O + NaOD, 125 MHz)

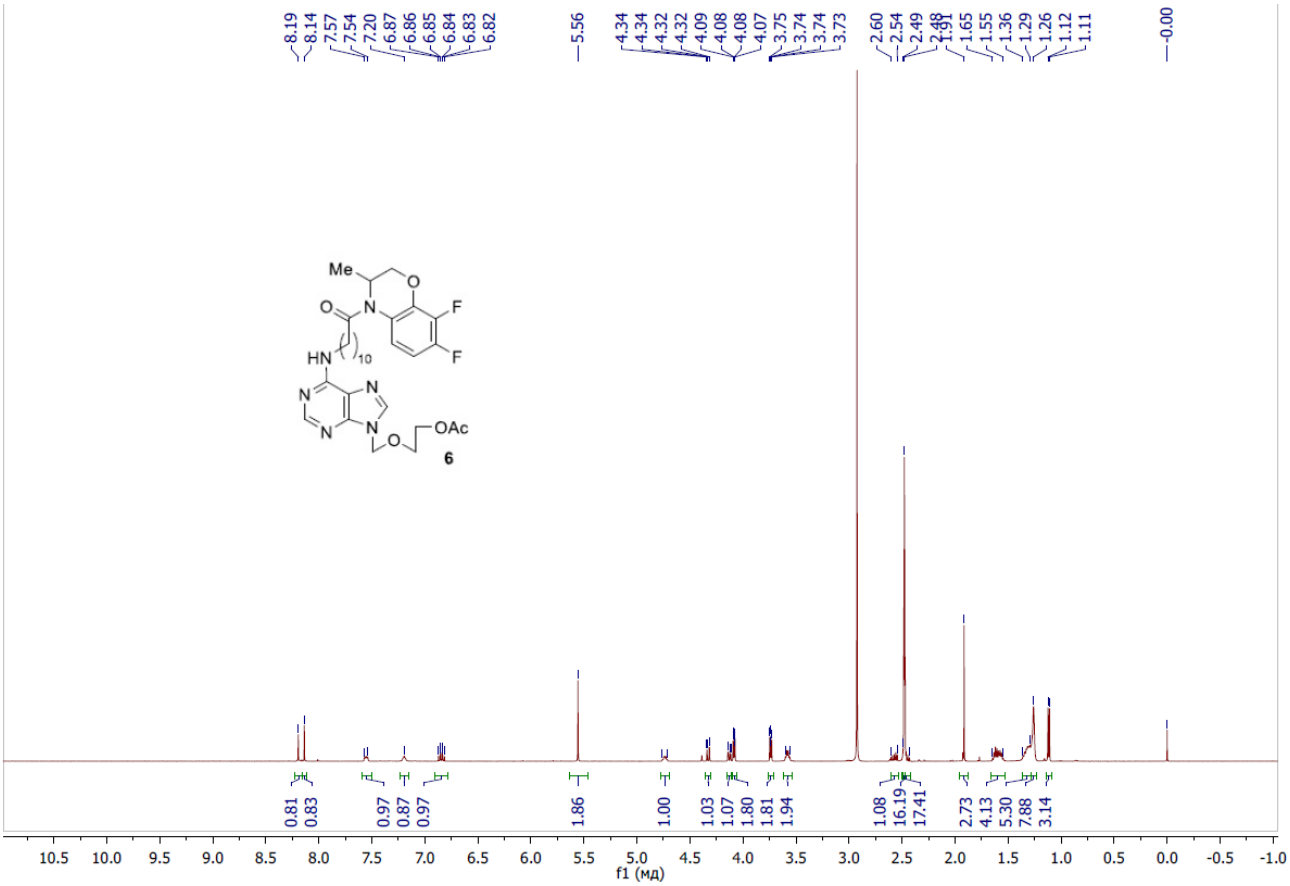

Figure S7. ^{1}H NMR spectrum of compound **6** (DMSO-d_6, 100 °C, 500 MHz)

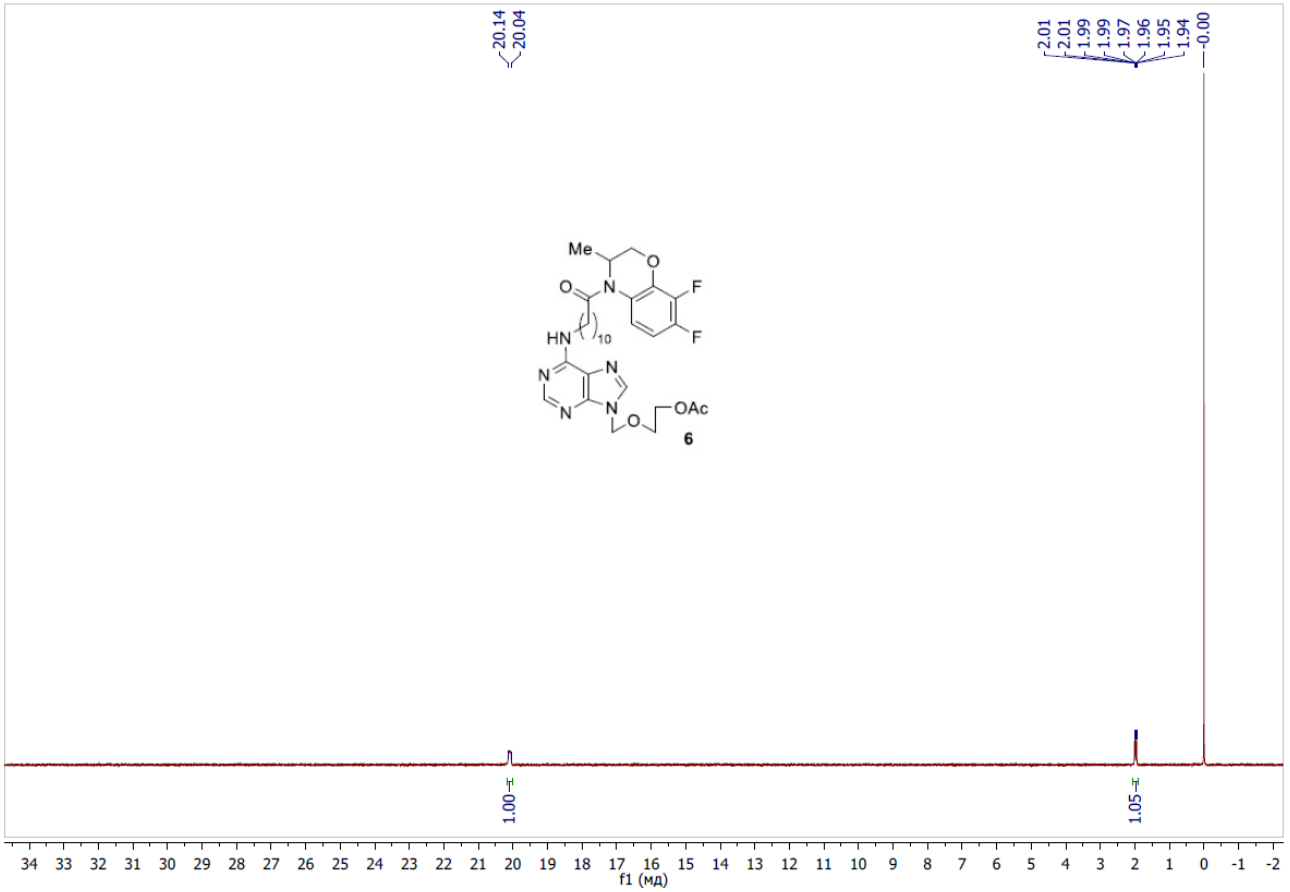

Figure S8. ^{19}F NMR spectrum of compound **6** (DMSO-d_6, 100 °C, 470 MHz)

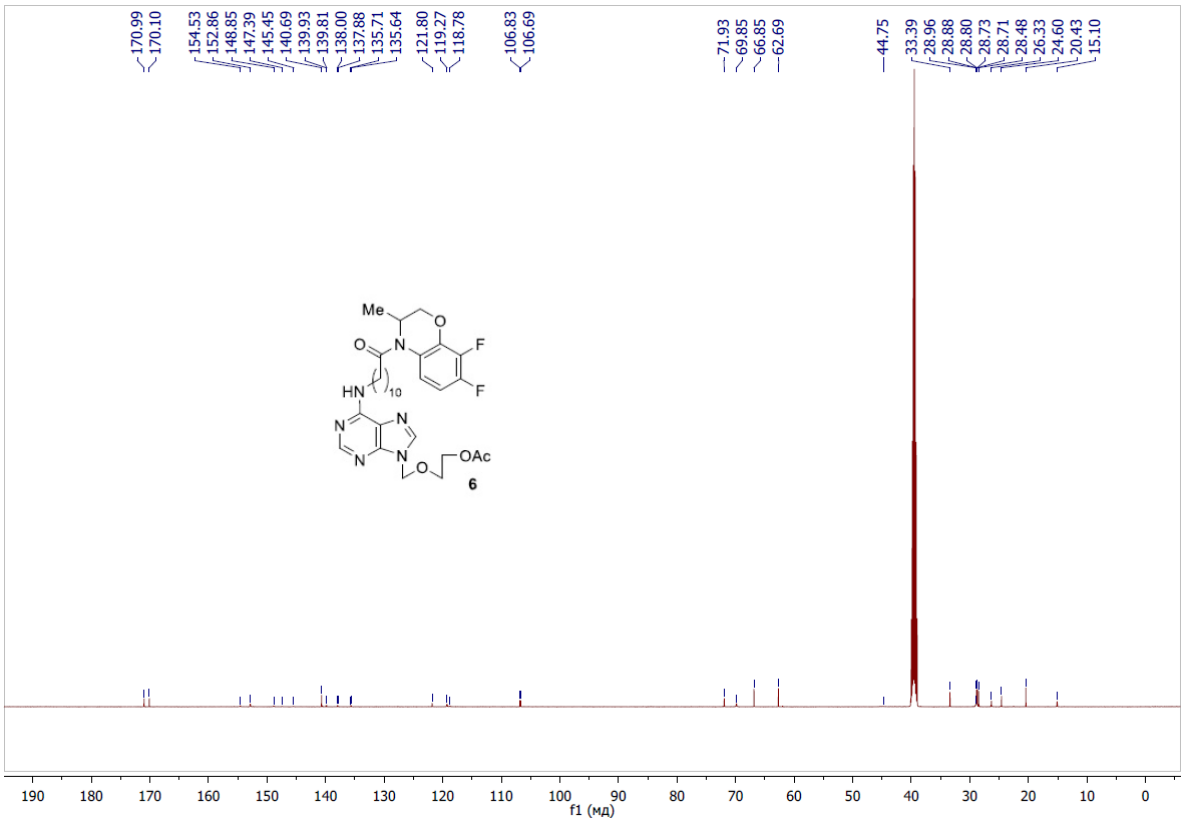

Figure S9. ^{13}C NMR spectrum of compound **6** (DMSO-d_6, 125 MHz)

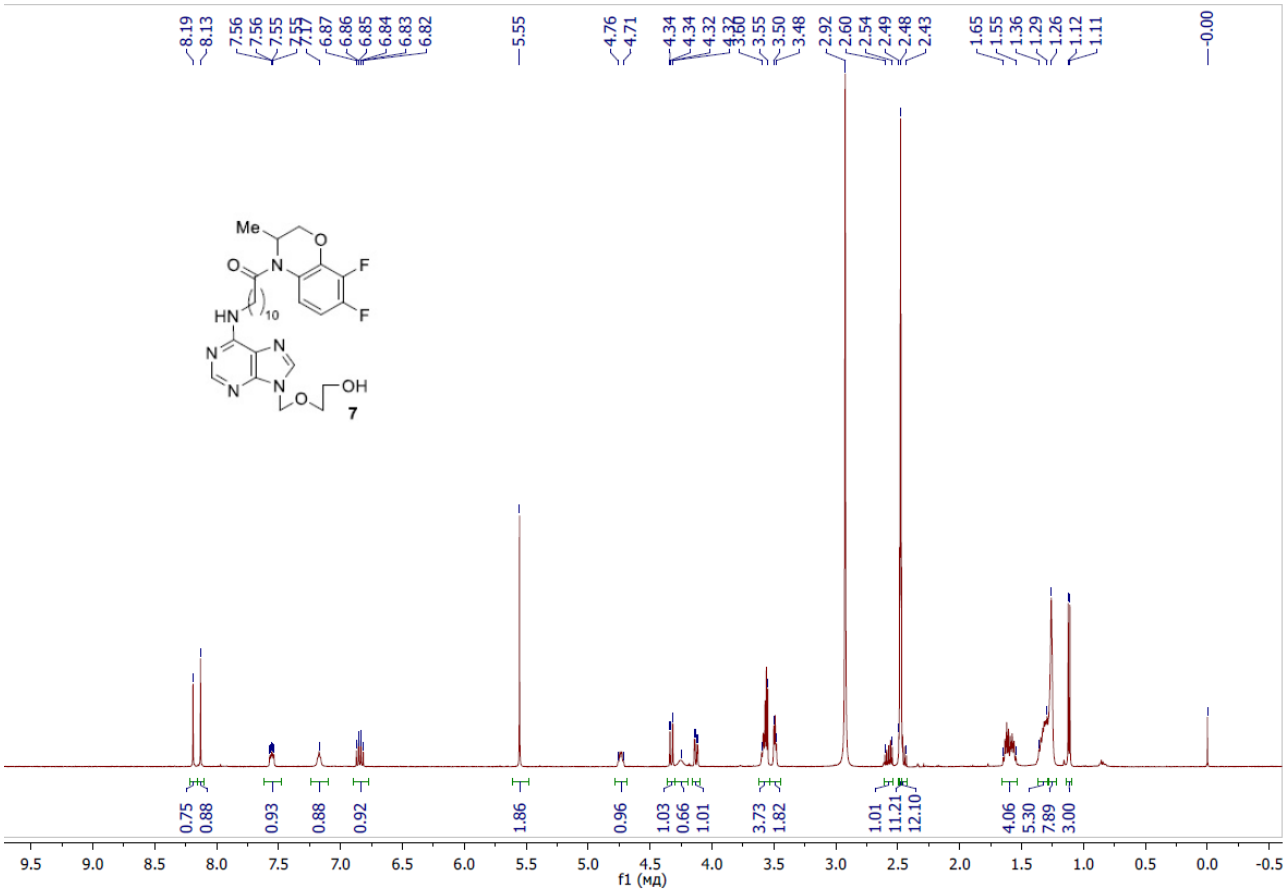

Figure S10. ^{1}H NMR spectrum of compound **7** (DMSO-d_6, 100 °C, 500 MHz)

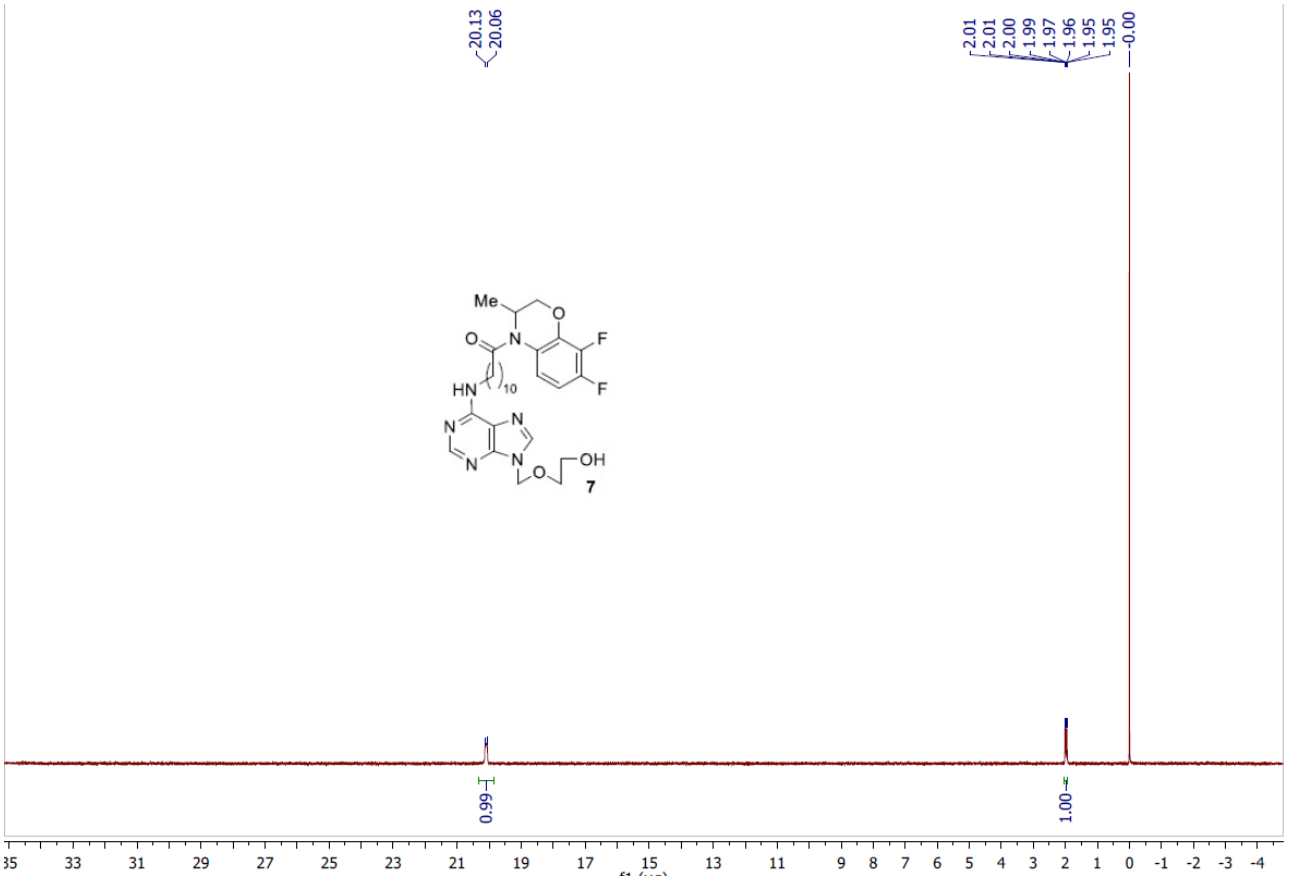

Figure S11. ^{19}F NMR spectrum of compound **7** (DMSO-d_6, 100 °C, 470 MHz)

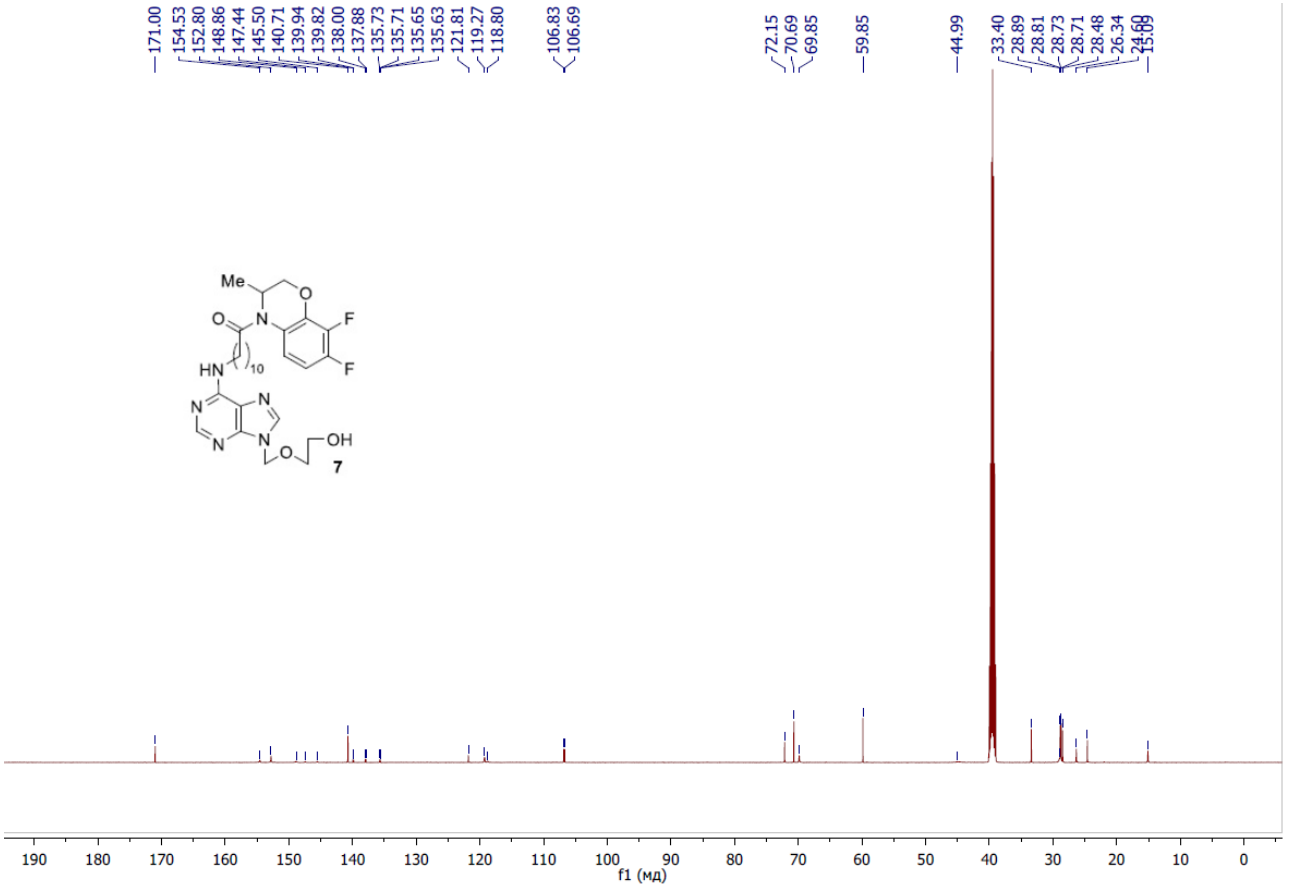

Figure S12. ^{13}C NMR spectrum of compound **7** (DMSO-d_6, 125 MHz)

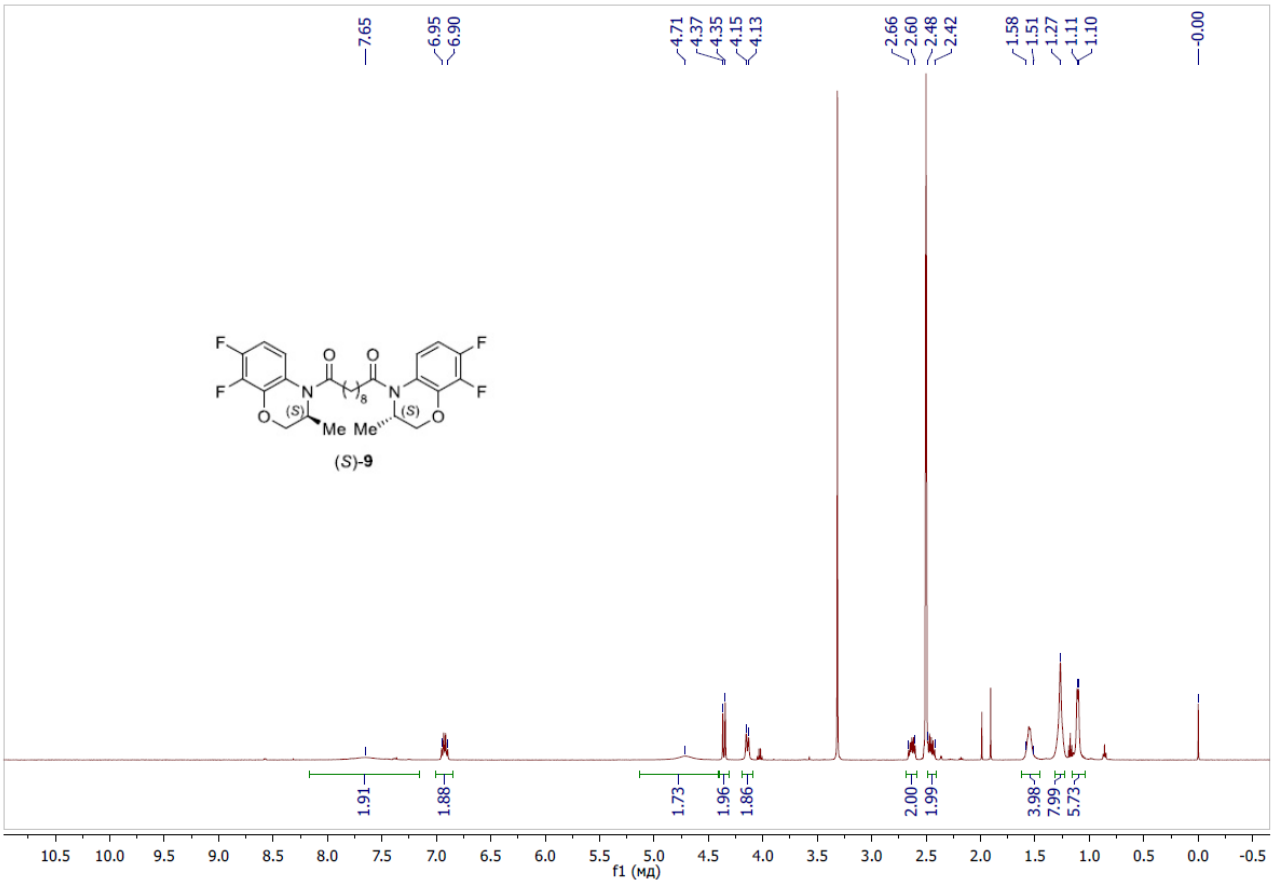

Figure S13. ^{1}H NMR spectrum of compound (*S*)-**9** (DMSO-d_6, 500 MHz)

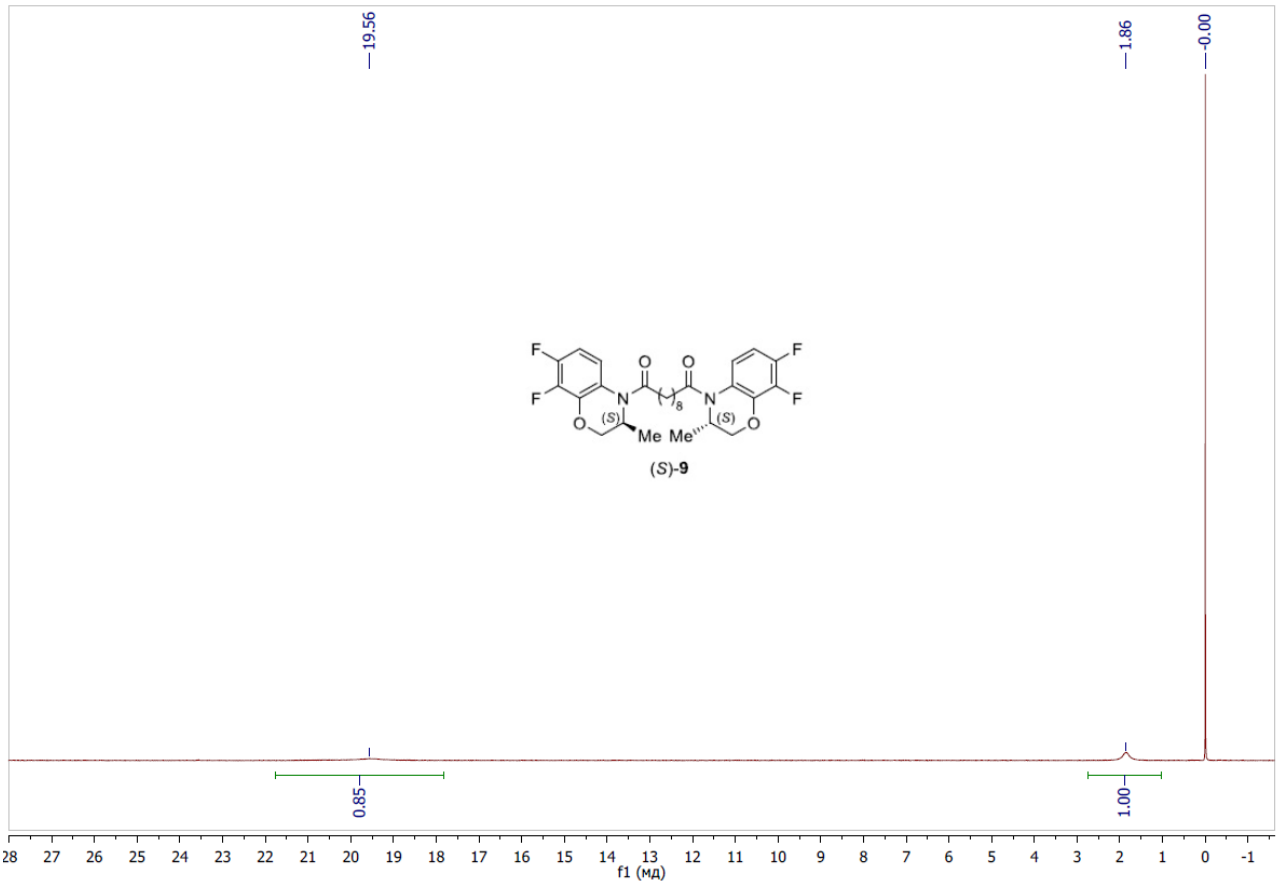

Figure S14. ^{19}F NMR spectrum of compound (*S*)-**9** (DMSO-d_6, 470 MHz)

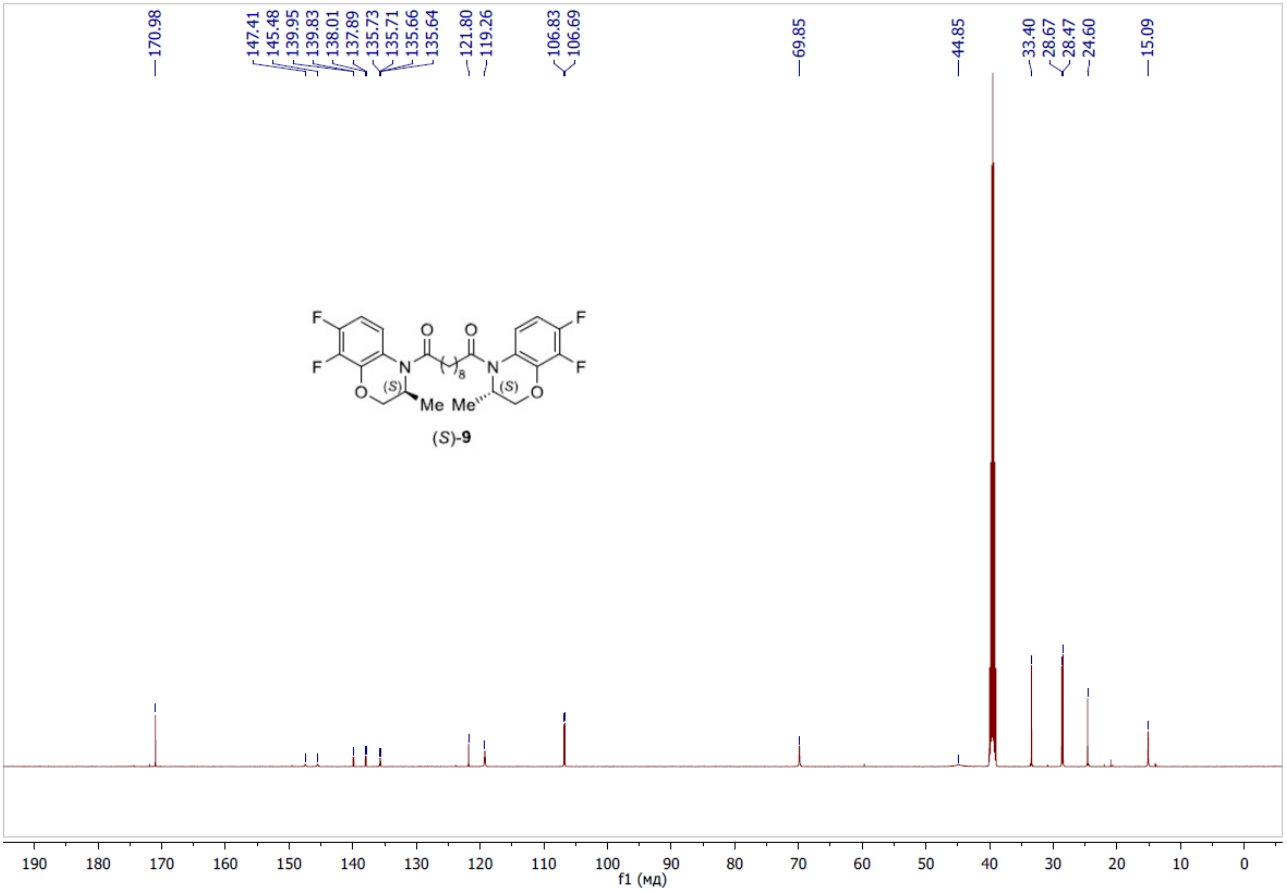

Figure S15. ^{13}C NMR spectrum of compound (*S*)-**9** (DMSO-d_6, 125 MHz)

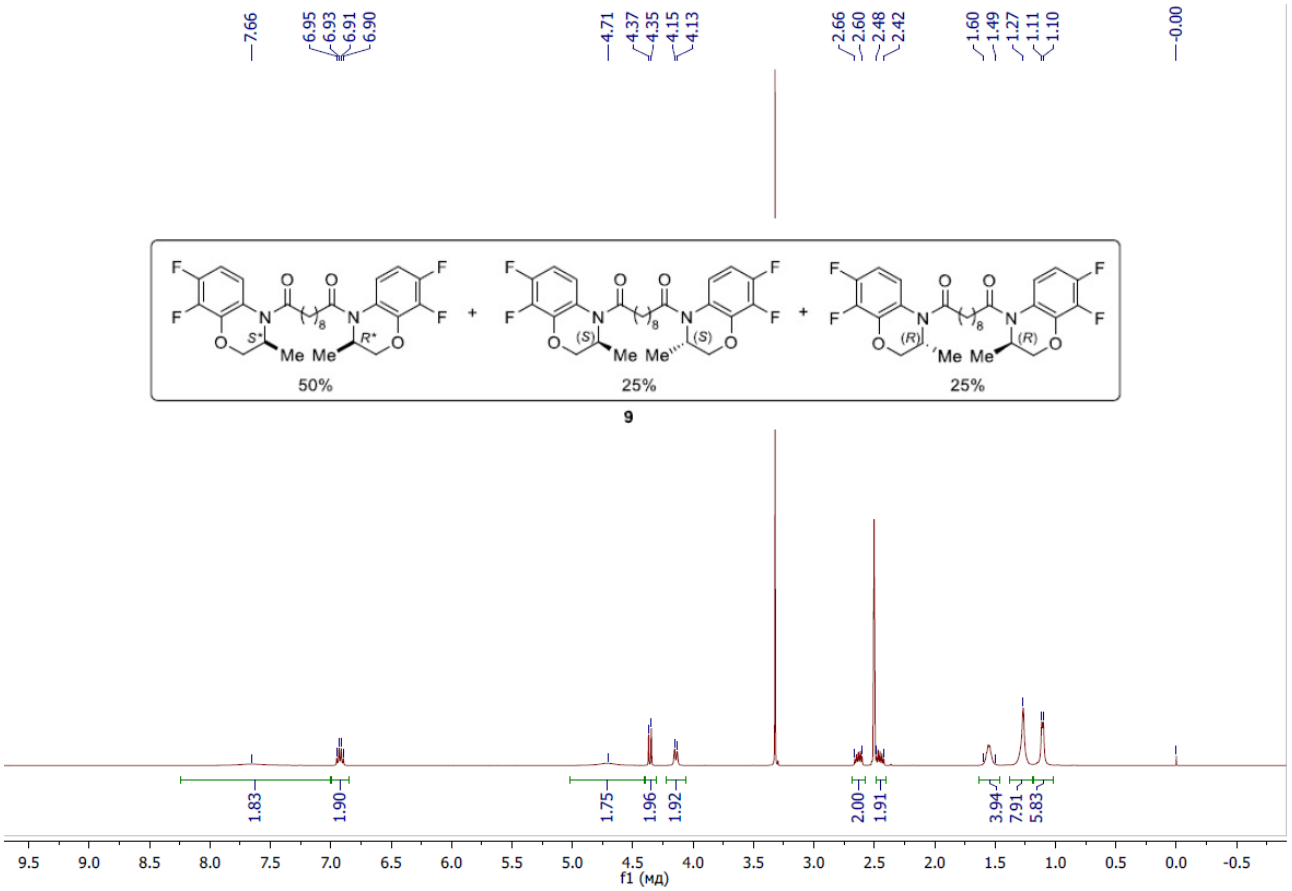

Figure S16. ^{1}H NMR spectrum of compound **9** (DMSO-d_6, 500 MHz)

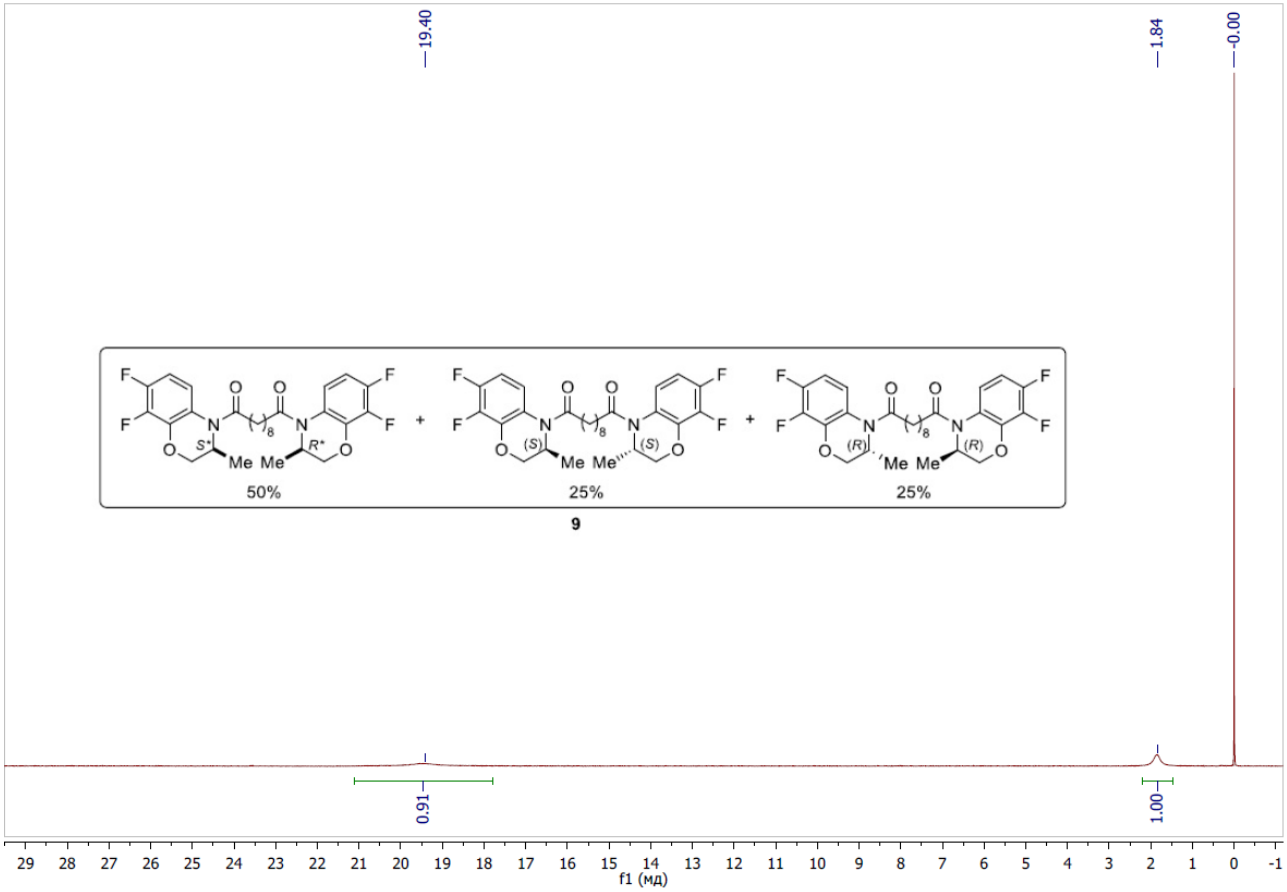

Figure S17. ^{19}F NMR spectrum of compound **9** (DMSO-d_6, 470 MHz)

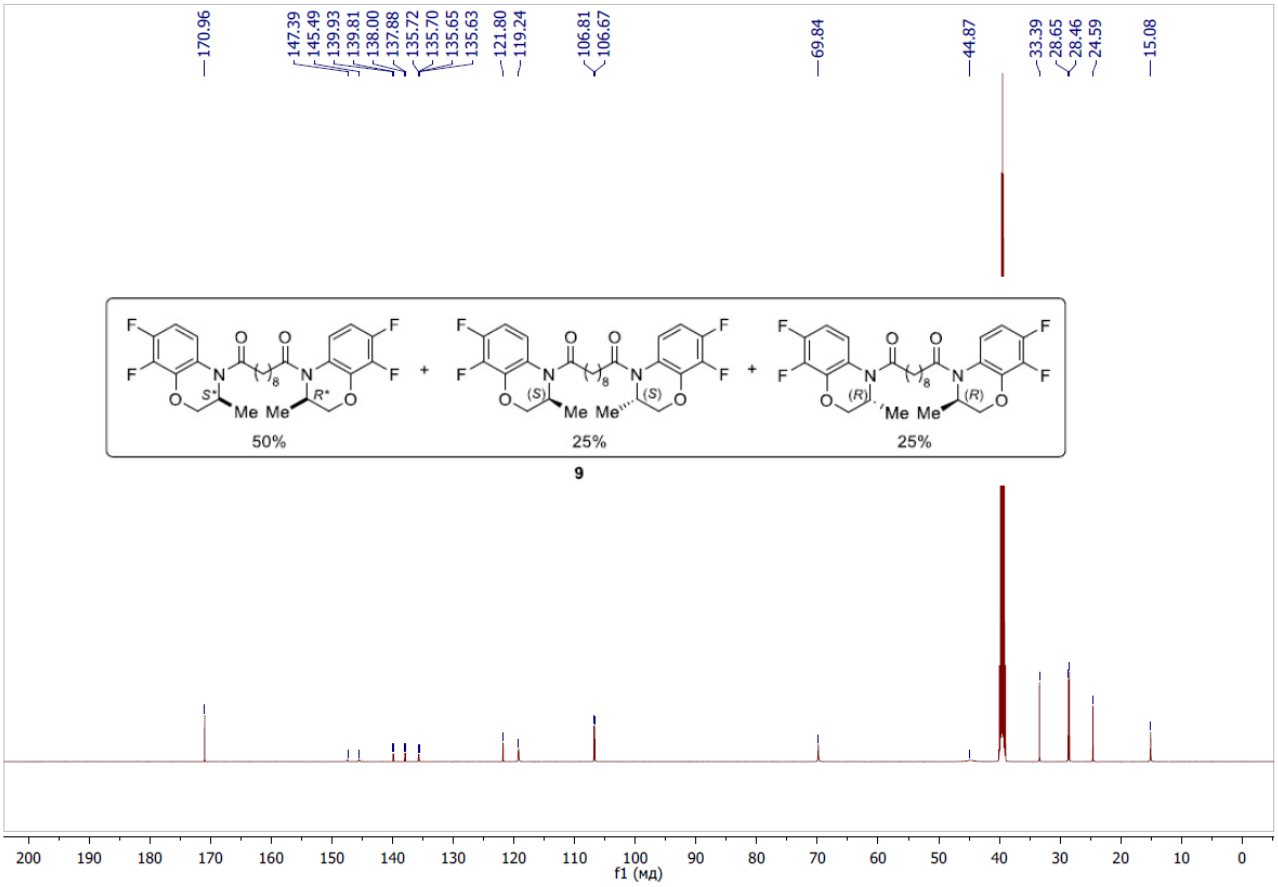

Figure S18. ^{13}C NMR spectrum of compound **9** (DMSO-d_6, 125 MHz)

HPLC Data

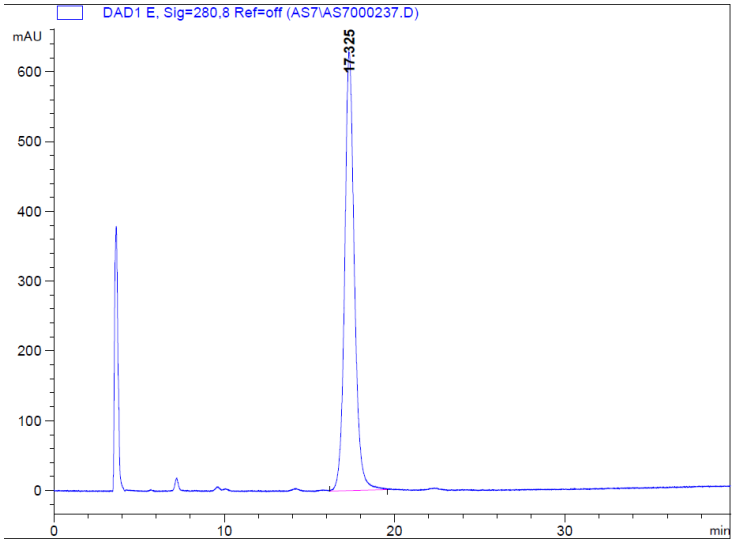

Peak #	RetTime [min]	Type	Width [min]	Area [mAU*s]	Height [mAU]	Area %
1	17.325	BB	0.5506	2.49048e4	628.14355	100.0000
Totals :				2.49048e4	628.14355	

Figure S19. HPLC of compound (*S*)-**9** ((S,S)-Whelk-O1, MeOH–H_2O 85 : 15, 0.8 mL/min; detection at 280 nm): *t* 17.3 min.

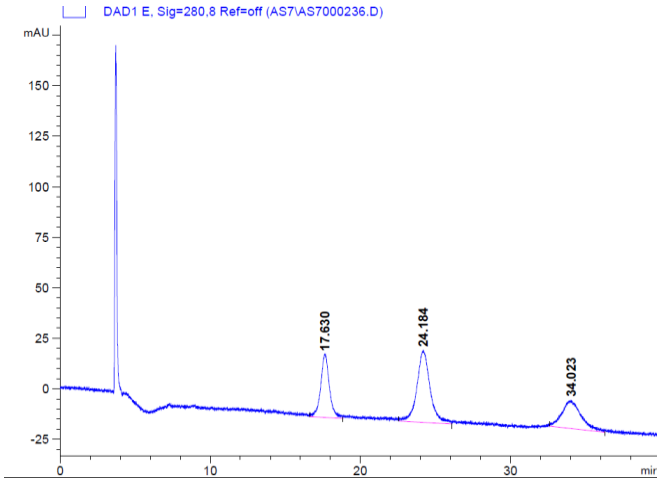

Peak #	RetTime [min]	Type	Width [min]	Area [mAU*s]	Height [mAU]	Area %
1	17.630	BV	0.4958	1267.48206	31.08143	27.1357
2	24.184	BB	0.7476	2180.08521	35.54097	46.6737
3	34.023	BV	1.0600	1223.34167	13.88373	26.1907
Totals :				4670.90894	80.50612	

Figure S20. HPLC of mixture of diastereomers **9** ((S,S)-Whelk-O1, MeOH–H_2O 85 : 15, 0.8 mL/min, detection at 280 nm): $t_{S,S}$ 17.6 min (27%), t_{R^*,S^*} 24.2 min (47%), $t_{R,R}$ 34.0 min (26%).

Cytotoxicity Assessment

Table S1. Cell lines and composition of culture medium

Cell line	Composition of complete culture medium
CT-26 murine colon carcinoma	RPMI-1640 supplemented with 100 × Glutamax, 100 × Penicillin-Streptomycin, 10% FBS, 0.1 M HEPES
4T1 murine mammary carcinoma	DMEM/F12 (4.5 mg/L glucose, 25 mM HEPES), 100 × Glutamax, 100 × Penicillin-Streptomycin, 10% FBS
MDA-MB-231 human breast adenocarcinoma	DMEM/F12 (4.5 mg/L glucose, 25 mM HEPES), 100 × Glutamax, 100 × Penicillin-Streptomycin, 10% FBS
COLO201 human colorectal adenocarcinoma	RPMI-1640, 100 × Glutamax, 100 × Penicillin-Streptomycin, 10% FBS
HepG2 human hepatocellular carcinoma	DMEM/F12 (4.5 mg/L glucose, 25 mM HEPES), 100 × Glutamax, 100 × Penicillin-Streptomycin, 10% FBS
A549 human non-small-cell lung carcinoma	RPMI-1640 supplemented with 10% FBS, 2mM L-glutamine and 100 × Penicillin-Streptomycin
SK-BR-3 human breast adenocarcinoma	RPMI-1640 supplemented with 10% FBS, 2mM L-glutamine and 100 × Penicillin-Streptomycin
SNU-1 human gastric carcinoma	RPMI-1640 supplemented with 10% FBS, 2mM L-glutamine and 100 × Penicillin-Streptomycin
Jurkat human acute T-lymphoblastic leukemia	RPMI-1640 supplemented with 10% FBS, 2mM L-glutamine and 100 × Penicillin-Streptomycin
WI-38 human lung fibroblasts	RPMI-1640 supplemented with 10% FBS, 2mM L-glutamine and 100 × Penicillin-Streptomycin

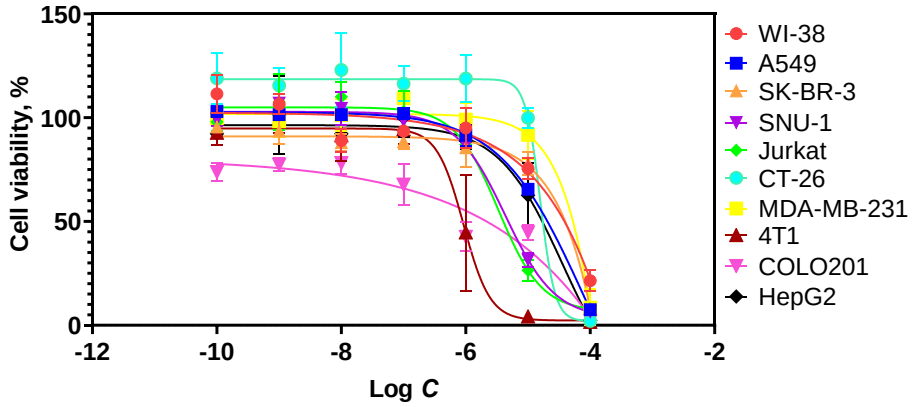

Figure S21. Viability of WI-38, A549, SK-BR-3, SNU-1, Jurkat, CT-26, MDA-MB-231, 4T1, COLO201, HepG2 cells *vs.* logarithmic concentration of compound **1c** after a 72-h incubation.

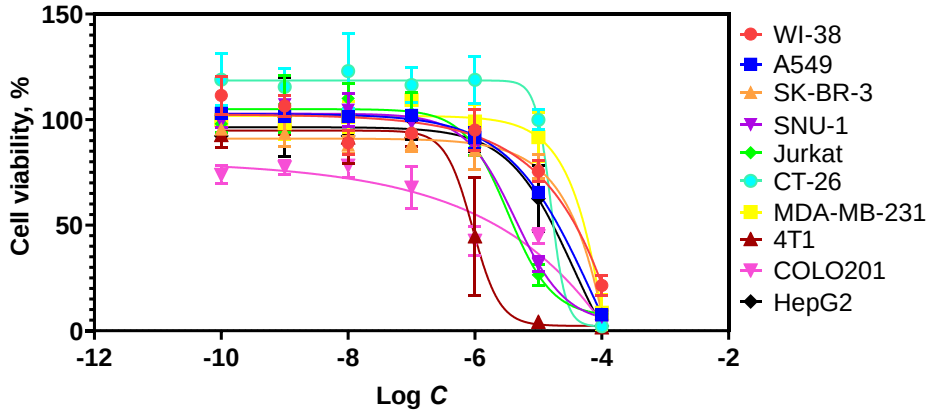

Figure S22. Viability of WI-38, A549, SK-BR-3, SNU-1, Jurkat, CT-26, MDA-MB-231, 4T1, COLO201, HepG2 cells *vs.* logarithmic concentration of compound **1d** after a 72-h incubation.

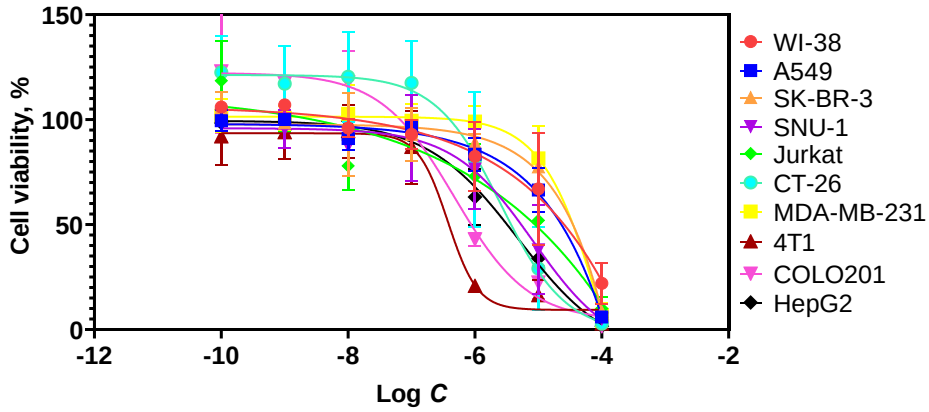

Figure S23. Viability of WI-38, A549, SK-BR-3, SNU-1, Jurkat, CT-26, MDA-MB-231, 4T1, COLO201, HepG2 cells *vs.* logarithmic concentration of compound **1e** after a 72-h incubation.

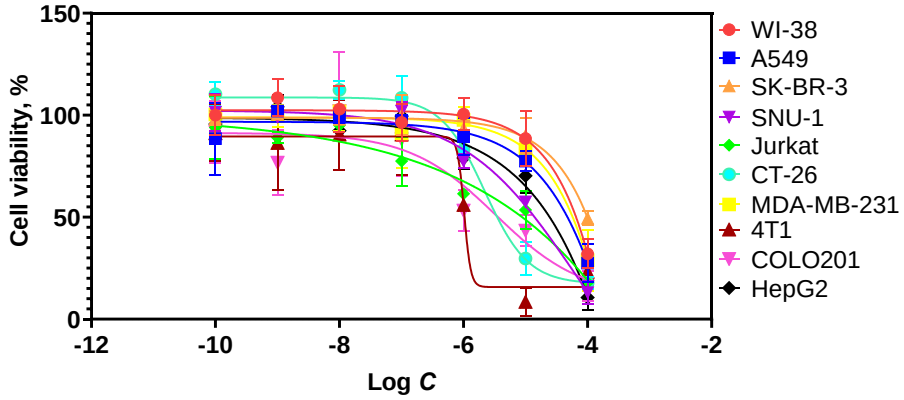

Figure S24. Viability of WI-38, A549, SK-BR-3, SNU-1, Jurkat, CT-26, MDA-MB-231, 4T1, COLO201, HepG2 cells *vs.* logarithmic concentration of compound **1f** after a 72-h incubation.

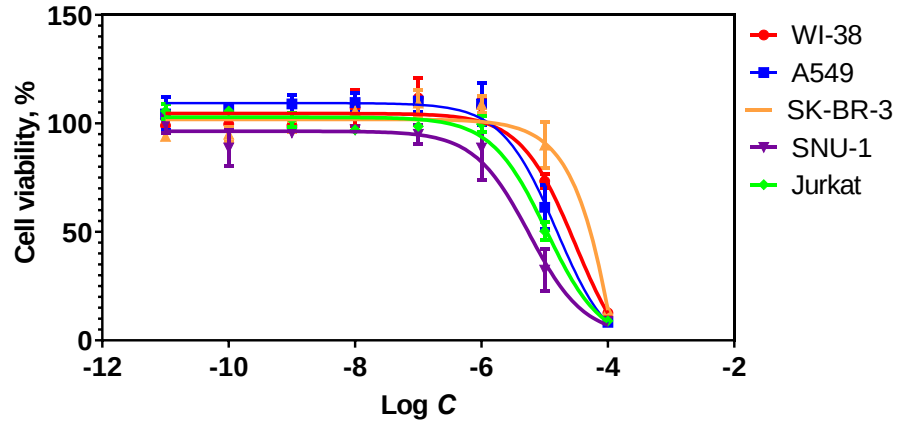

Figure S25. Viability of WI-38, A549, SK-BR-3, SNU-1, and Jurkat cells *vs.* logarithmic concentration of compound **6** after a 72-h incubation.

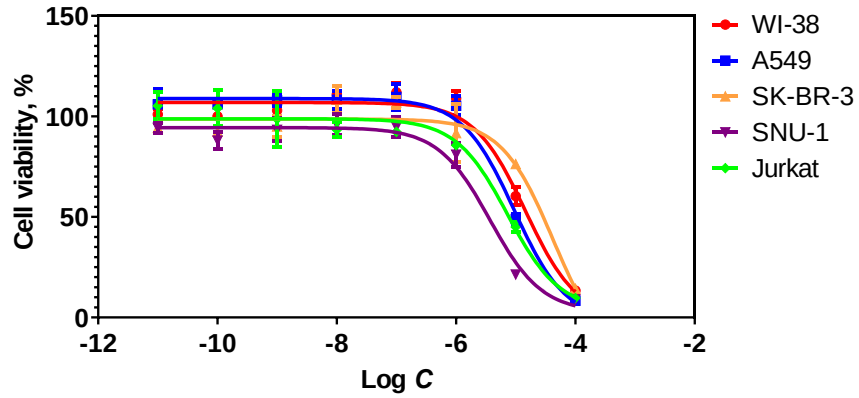

Figure S26. Viability of WI-38, A549, SK-BR-3, SNU-1, and Jurkat cells *vs.* logarithmic concentration of compound **7** after a 72-h incubation.

Cell Cycle Analysis

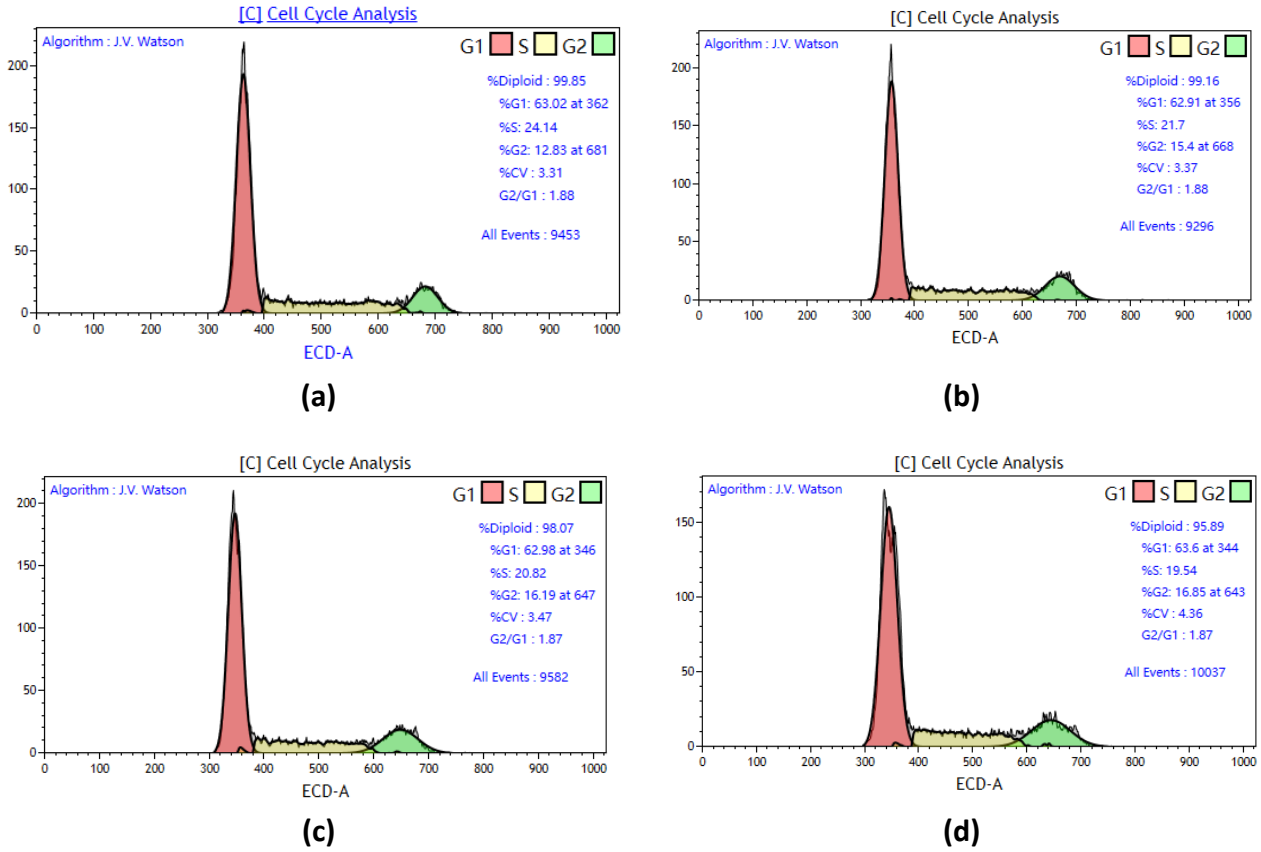

Figure S27. Diagrams of the COLO201 cell distribution by cell cycle phases: (**a**) without the addition of the test compound (control) and after 24-h incubation with compound **1d** at concentrations of (**b**) 0.9×10^{-6} M, (**c**) 1×10^{-6} M, and (**d**) 2×10^{-6} M.

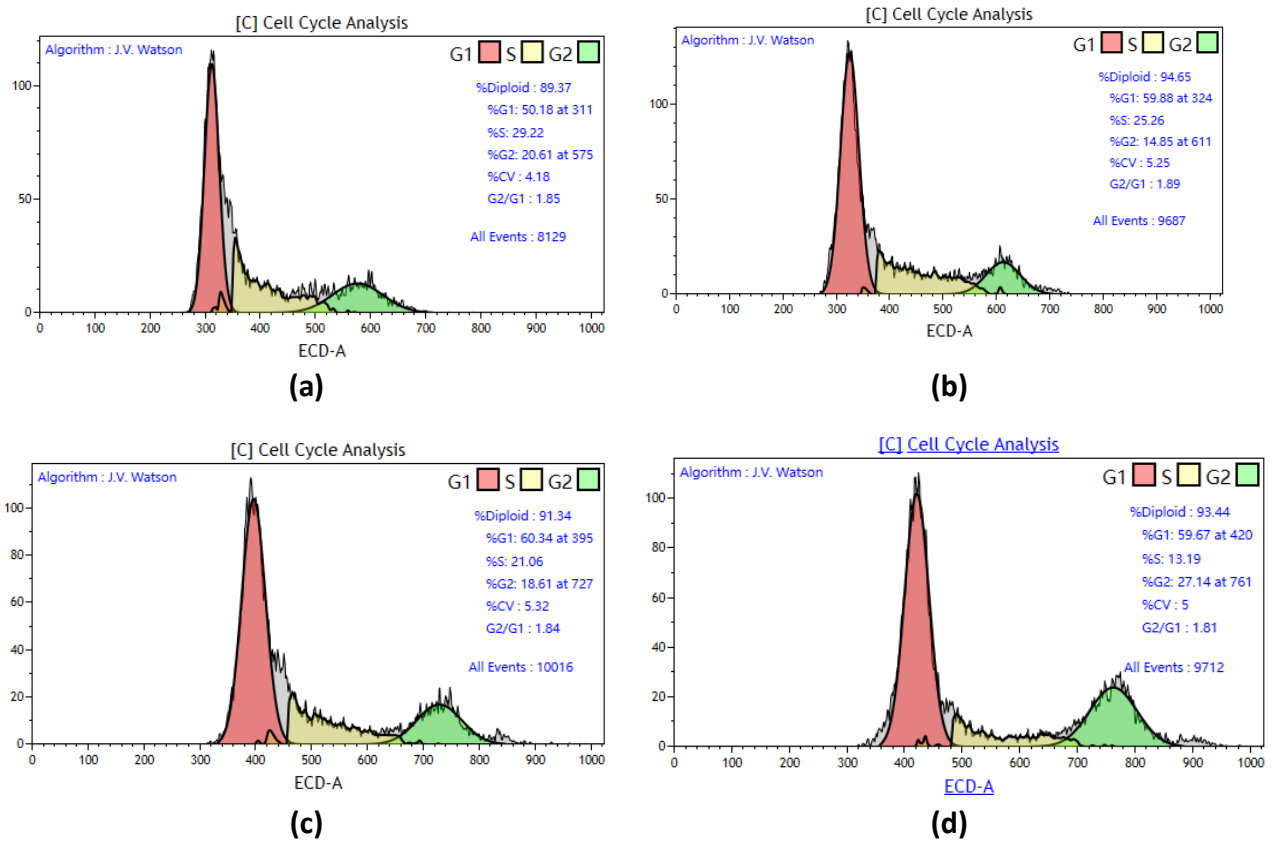

Figure S28. Diagrams of the MDA-MB-231 cell distribution by cell cycle phases: (**a**) without the addition of the test compound (control) and after 24-h incubation with compound **1d** at concentrations of (**b**) 10×10^{-6} M, (**c**) 20×10^{-6} M, and (**d**) 30×10^{-6} M.

Table S2. Effect of compound **1d** on the cell cycle of the COLO201 cells. Data are presented as $M \pm$ SD ($n = 3$).

Concentration (M)	Number of cells (%) in cell cycle phase			Cell proliferation index (%)
	G0/G1	S	G2M	
0	63.38±2.16	24.64±1.24	11.98±1.23	36.62±2.16
0.9×10^{-6}	62.95±0.21	21.35±0.34*	15.70±0.45*	37.05±0.21
1×10^{-6}	63.21±0.29	21.38±0.70*	15.41±0.74*	36.78±0.29
2×10^{-6}	64.60±0.97	18.51±0.99*	16.84±0.08*	35.35±0.96

* $p < 0.05$ compared to control.

Table S3. Effect of compound **1d** on the cell cycle of the MDA-MB-231 cells. Data are presented as $M \pm$ SD ($n = 3$).

Concentration (M)	Number of cells (%) in cell cycle phase			Cell proliferation index (%)
	G0/G1	S	G2M	
0	48.01±1.94	31.22±1.81	20.78±1.00	52.00±1.94
10×10^{-6}	60.92±0.91*	25.33±0.42*	13.74±1.13*	39.08±0.91*
20×10^{-6}	62.13±1.98*	20.52±0.81*	17.05±1.36*	37.57±1.98*
30×10^{-6}	59.37±1.02*	13.13±0.21*	27.49±1.22*	40.63±1.01*

* $p < 0.05$ compared to control.